Cascade architecture for nonlinear control of transient and stationary regimes of friction-induced vibrations

Lyes Nechak, Pascal Morin

Cascade architecture for nonlinear control of transient and stationary regimes of friction-induced vibrations

Lyes Nechak[1] and Pascal Morin[2]

L. Nechak is with Laboratoire de Trobologie et Dynamique de systèmes, Rue Guy de Collogue, Ecully, 69132, France, lyes.nechak@ec-lyon.fr

P. Morin is with Institut des Systèmes Intelligents et de Robotique (ISIR), Sorbonne Université, CNRS, UMR 7222, Paris, 75005, France, pascal.morin@sorbonne-universite.fr

January 15, 2023

Abstract

This paper presents a new control approach for mitigating Friction-Induced Vibration (FIV) issued from the mode-coupling mechanism. The key idea is to put the friction system onto a cascade of independent subsystems by using a first stage control. Then, a second stage control is defined and proven to be much more efficient for controlling both the transient and stationary regimes of the FIV. Asymptotic stabilization is formally demonstrated for the whole control scheme. Moreover, by numerical simulations, it is shown that the performances of the closed loop systems present an interesting robustness with respect to parameter uncertainty and to the saturation phenomenon which opens up promising practical perspectives for the proposed control technique.

1 Introduction

Because of their negative impact, friction-induced vibrations (FIV) have received a lot of attention in the last decades as evidenced by the significant amount of experimental and numerical works related to engineering and industry applications [19, 50, 2]. Indeed, these vibrations, which appear in structures with friction interfaces, can be the cause of numerous undesirable phenomena such as noise in braking, clutch or wiping systems [22, 17, 1, 10], and loss of performances in positioning systems, which manifests itself in larger steady- state positioning error and settling time [7, 48, 13, 59]. They can also induce phenomena of fatigue and wear that can lead to the system breakdown. Hence, it is very important to be able to predict and analyze them in order to anticipate and implement solutions that will reduce or even eliminate them [54, 33, 9].

Nowadays, it is common to classify the mechanisms generating FIV from tribological and structural viewpoints [24, 25, 40]. If the tribological mechanism relates the generation of vibrations to the continuous or discontinuous variation of the friction coefficient against the relative sliding speed [24, 25, 55], the structural mechanism rather indicates the geometrical aspects inducing the coupling of the normal degrees of freedom with the tangential degrees of freedom of contact as being at the origin of the vibrations [49, 24, 25, 52]. The coupling in question is characterized by the so-called 'modes coalescence' which consists of the bringing together of two natural frequencies (imaginary parts of some couple of the system eigenvalues) according to the friction coefficient up to the coalescence point where the frequencies become equal while the corresponding real parts separate. One real part becoming positive will induce a self-sustaining vibration when the static equilibrium of the system is disturbed.

Numerous strategies including passive and active approaches have been proposed for mitigating FIV. Passive approaches are in a way empirical since they are based on the adjustment of the system parameters or the parameter of an added subsystem (as a absorber or a Nonlinear Energy Sink (NES)) without any external power supply so as to obtain suitable dynamic properties [46, 31, 15, 6, 30, 47]. The active one proceeds by introducing external support in order to act on the damping properties and/or to compensate friction effects [5, 39, 58]. In this framework, numerous controllers have been proposed. The Proportional-Integral-Derivative (PID) regulator can be mentioned as the most classical one, proposed for controlling FIV for example in [4, 51]. More efficiency was shown for the PID when associated with the active force control (AFC) in [53]. Linear delayed and non-delayed state feedbacks were also proposed in [32, 3, 26, 16, 38] while nonlinear techniques exploiting the full and partially linearizing state feedbacks were exploited in [42, 43] and combined with the receptance method in [11] for the active controlling of FIV. In [21], a control scheme which consists of a combination of a parallel feed-forward compensator (PFC) with an adaptive λ-tracking feedback control is proposed for controlling friction-induced self-excited oscillations in a two-mass electromechanical system with an elastic shaft and a friction load with a Stribeck effect. Otherwise, mitigating FIV by ensuring robustness levels with respect to uncertainty was also addressed in [57] and in [44, 37].

Most of the recorded studies about FIVs mitigating have focused on reducing or suppressing the amplitude of the steady vibration regardless of the properties of the corresponding transient regime such as the amplitude and the settling time. A more damped and fast transient is often paid by high amplitude for the control inputs which, not to mention the energy cost, leads to saturation phenomena [14, 12]. This paper deals with this issue and proposes a new approach for mitigating both the mode-coupling based steady and transient friction-induced vibrations by considering minimal models representing mode-coupling instabilities occurring in friction systems as drum brake systems [22].

Behind the use of minimal models, there is the aim to overcome the numerical difficulties occasioned by large dimension patterns that prevent a suitable objective analysis of the feasibility and efficiency of the new proposed approach. These minimal models give the key advantage to faithfully represent the mechanism generating friction-induced vibrations through considering mechanical systems with small numbers of degree-of-freedom. Numerous studies have developed such models within different frameworks especially the brake squeal framework, by considering different objectives namely the analysis and prediction [23, 28, 29, 41, 56], the uncertainty propagation [20, 60, 35], and passive and active control [46, 8, 53, 42, 43].

This study investigates the potential of a new nonlinear control scheme for mitigating mode-coupling based friction-induced vibrations. More precisely, the objective is to obtain both global asymptotic stability of the closed-loop system and good transient characteristics. The proposed approach is developed by considering minimal models of mode-coupling phenomenon, such as the Hultèn model [23] and the Hoffman-like model [11]. The main idea is to transform the control system into a cascade structure, via a preliminary feedback control action. The cascade structure can then be exploited for transient characteristics' tuning. A particular advantage of this approach is related to the system's natural frequencies that are kept unchanged by the state feedback. A comparison with the linearizing state feedback approach by numerical simulations shows a great advantage of this new approach for controlling the transient behavior with an interesting compromise between the damping ratio and the control amplitude. Otherwise, the control performances of the proposed cascade architecture based control prove to be robust with respect to severe control saturation.

2 Problem statement

We are interested by mechanical systems submitted to friction-induced vibrations and described by second order differential equations given by

$$\mathrm{M}\ddot{\mathrm{X}} + \mathrm{C}\dot{\mathrm{X}} + \mathrm{KX} + \mathrm{F_{NL}}(\mathrm{X}) = \mathrm{Bu}(t) \tag{1}$$

where X, $\dot{\mathrm{X}}$, and $\ddot{\mathrm{X}}$ denote respectively the displacement vector and the associated velocity and acceleration vectors, all belonging to $\mathbb{R}^N$ with N the system's number of degrees of freedom. The control input is $\mathrm{u} \in \mathbb{R}^p$ and B is the associated control matrix. M, C, and K respectively denote the mass matrix, damping matrix, and stiffness matrix. $\mathrm{F_{NL}}$ is a smooth nonlinear function (representing in the study framework nonlinear contact and friction forces).

Let $x = (\mathrm{X}', \dot{\mathrm{X}}')'$ denote the state vector associated with System (1). Assuming, without loss of generality, that $\mathrm{F_{NL}}(0) = 0$, then $x = (0, 0)'$ is an equilibrium of System (1) for the control $u \equiv 0$. The control

objective is to determine a nonlinear state feedback control $\mathrm{u}(t) = \boldsymbol{\gamma}(x(t))$ in order to make this equilibrium asymptotically stable while ensuring suitable transient properties (in terms of vibration amplitude).

As previously mentioned, a new nonlinear control scheme is proposed in this study. It exploits the possibility to put the system into a cascade form by a preliminary decoupling control action. Then, the decoupled structure gives a more suitable framework to stabilize and suppress the FIV with the possibility to better monitor the transient regime. In order to present the proposed method, two minimal models are exploited in the following sections. Firstly the control of the Hultèn model [23] is considered. Secondly, extension of the approach to a higher order model (the Hoffman-like system [11]) is proposed.

3 Control of the Hultèn model

The Hultèn model [23], represented on Figure (1), was shown to faithfully represent the mode-coupling phenomenon occurring in drum brake systems. It was considered in numerous studies, as in [27] for the understanding of the role of damping in mode-coupling, in [36, 18] for uncertainty propagation and quantification, in [6, 42] for mitigating mode-coupling instabilities, and recently in [43] for the control of mode-coupling based vibrations by using nonlinear state observers. It is considered in this section in order to assess the performances of the proposed control scheme for mitigating FIV issued from the mode-coupling mechanism.

The mechanical system consists of a mass assumed to be in a permanent contact with a moving band. The contacts are modelled by two stiffnesses with linear and nonlinear (cubic) parts. The friction coefficient μ at the contact is assumed to be constant as well as the velocity of the band. The relative velocity between the band and the velocities $\dot{X}_1$ and $\dot{X}_2$ is assumed positive which makes constant the direction of the friction force. According to the Coulomb's law, the tangential force F_{T} is assumed to be proportional to the normal force F_{N}, i.e., $F_{\mathrm{T}} = \mu F_{\mathrm{N}}$. The system is governed by second-order differential equations as given by (1) with the following standardized matrices:

$$\mathrm{M} = \begin{bmatrix} m & 0 \\ 0 & m \end{bmatrix},\ \mathrm{C} = \begin{bmatrix} c_1 & 0 \\ 0 & c_2 \end{bmatrix},\ \mathrm{K} = \begin{bmatrix} k_1 & -\mu k_2 \\ \mu k_1 & k_2 \end{bmatrix},\ \mathrm{B} = \begin{bmatrix} 0 \\ 1 \end{bmatrix},$$

and

$$\mathrm{F_{NL}}(X) = \begin{bmatrix} k_1^{NL} X_1^3 - \mu k_2^{NL} X_2^3 \\ \mu k_1^{NL} X_1^3 + k_2^{NL} X_2^3 \end{bmatrix}$$

The system can be reformulated by introducing the relative damping coefficients $\eta_i = c_i/\sqrt{m k_i}$ and the natural pulsations $w_i = \sqrt{k_i/m}$ as follows:

$$\begin{cases} \ddot{X}_1 = -w_1^2 X_1 - \eta_1 w_1 \dot{X}_1 + \mu w_2^2 X_2 - \psi_1^{\mathrm{NL}} X_1^3 + \mu \psi_2^{\mathrm{NL}} X_2^3 \\ \ddot{X}_2 = -\mu w_1^2 X_1 - w_2^2 X_2 - \eta_2 w_2 \dot{X}_2 - \mu \psi_1^{\mathrm{NL}} X_1^3 - \psi_2^{\mathrm{NL}} X_2^3 + \frac{u}{m} \end{cases} \tag{2}$$

where $u \in \mathbb{R}$ is the system's control input and $\psi_i^{\mathrm{NL}} = \frac{k_i^{\mathrm{NL}}}{m}$, for $i = 1, 2$.

For numerical simulations, model parameters are given in SI by: $w_1 = 2\pi \times 100$ rad/s, $w_2 = 2\pi \times 75$ rad/s, $\eta_1 = \eta_2 = 0.02$, $\psi_1^{\mathrm{NL}} = w_1^2$, $\psi_2^{\mathrm{NL}} = 0$, $\mu = 0.4$ the nominal value of the friction coefficient, and $m = 1$ Kg.

3.1 Review of previous results

The Hultèn system was widely used and studied in the literature and is known to exhibit friction-induced vibrations due to the mode-coupling phenomenon shown in Figure (2). The frequencies approach each other as the friction coefficient μ increases until the coalescence point $\mu_c \approx 0.2893$ where the frequencies become equal while the real parts of the corresponding eigenvalues separate. One real part becoming positive makes the equilibrium unstable. Hence, a small perturbation on the system will make the system's state move far away from its equilibrium with a divergence rate defined by the eigenvalues' real parts, until an oscillating regime is reached. These oscillations must be suppressed or at least mitigated. Controlling these vibrations by using the nonlinear scheme based on state feedback linearization was considered in [42]. The principle was to apply a nonlinear state feedback that algebraically transforms the system into a linear one the

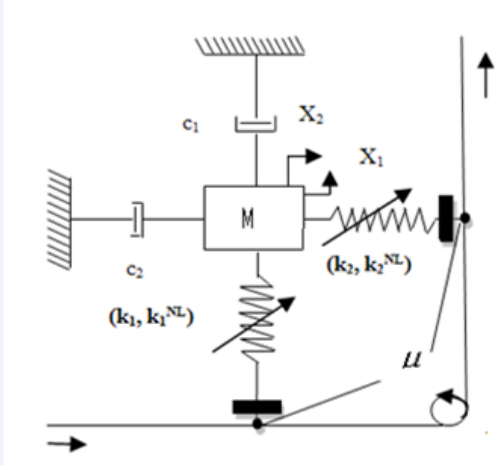

Figure 1: Mechanical system

dynamics of which is fixed by applying the classical pole placement approach. More precisely, the control law proposed in [42] is the nonlinear state feedback control :

$$u = \frac{m}{\mu w_2^2}\begin{pmatrix} -(x_2(\eta_1 w_1(w_1^2 + 3\psi_1^{\mathrm{NL}} x_1^2) - 6\psi_1^{\mathrm{NL}} x_1 x_2) + \\ (-\eta_1^2 w_1^2 + w_1^2 + 3\psi_1^{\mathrm{NL}} x_1^2)(w_1^2 x_1 + \eta_1 x_2 w_1 - \mu x_3 w_2^2 + \psi_1^{\mathrm{NL}} x_1^3) \\ -\mu w_2^2(\mu w_1^2 x_1 + x_3 w_2^2 + \eta_2 x_4 w_2 + \mu\psi_1 x_1^3) - \eta_1 \mu w_1 w_2^2 x_4) + v \end{pmatrix} \tag{3}$$

with

$$v = -k_0 z_1 - k_1 z_2 - k_2 z_3 - k_3 z_4 \tag{4}$$

where the z_i are the new coordinates defined by the diffeomorphism such that:

$$\begin{cases} z_1 = x_1 \\ z_2 = x_2 \\ z_3 = -w_1^2 x_1 - \eta_1 w_1 x_2 + \mu w_2^2 x_3 - \psi_1^{\mathrm{NL}} x_1^3 \\ z_4 = \eta_1 w_1^3 x_1 + \left(\eta_1^2 w_1^2 - w_1^2\right) x_2 - \eta_1 w_1 w_2^2 \mu x_3 + \mu w_2^2 x_4 + \eta_1 w_1 \psi_1^{\mathrm{NL}} x_1^3 \ldots \\ -3\psi_1^{\mathrm{NL}} x_2 x_1^2 \end{cases} \tag{5}$$

The dynamical behaviour of the system (2) is made asymptotically stable with transient properties depending on the location of the eigenvalues in the left half complex plane, given by the roots of the characteristic polynomial corresponding to (4). At this point, it is important to remark that the closed-loop dynamics of z is linear but, due to the fact that the diffeomorphism between z and the original state variable x is highly nonlinear, the closed-loop dynamics of x remains highly nonlinear. This is illustrated by the simulation results reported in Figure (3), which shows the open-loop response (black) and closed-loop (red) response for two different choices of control gains $k_0, \cdots, k_3$. The first choice of control gains (Figure (3)-(a,c)) shows weak damping of X_1's time response compared to the second choice (Figure (3)-(b,d)) for which the closed-loop eigenvalues have been placed further to the left. However, this is achieved at the price of large control amplitude (and thus control energy). Indeed, the control laws plotted in (3)-(e) and (3)-(f) well illustrate the well known relation between transient damping properties and the related control energy. A more damped transient requires a higher control energy. In practice however, high levels of control energy may lead to control saturation, which in turn can negatively impact the closed-loop performance. This dilemma between a damped transient and a reasonable level of the control energy needs to be addressed. This also motivates the development of the approach proposed in this paper.

3.2 Proposed approach

Compared to the feedback linearization recalled above, the present approach does not try to transform the system's dynamics into a linear system in new coordinates. Indeed, it is known that feedback linearization

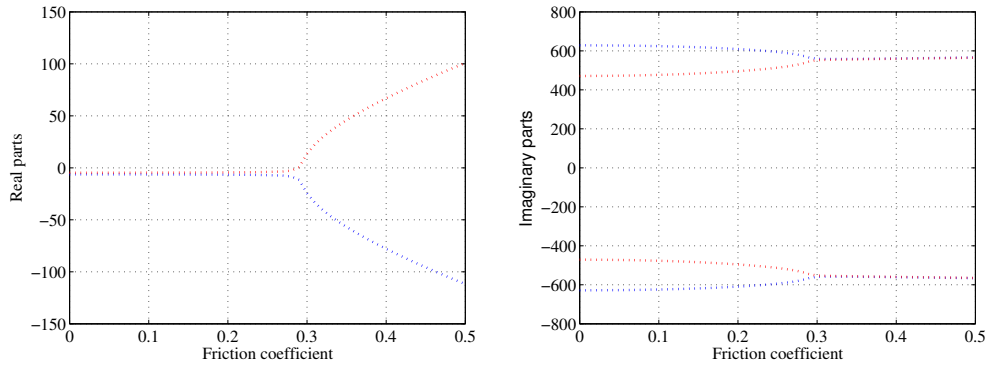

(a) (b)

Figure 2: Evolution of the eigenvalues of the Hultèn system linearized around the origin $\boldsymbol{x}_e = (\mathbf{0}, 0)$, versus the friction coefficient μ

sometimes leads to compensating in the control law dynamic effects that do not jeopardize stability, which can be both inefficient from a control energy point of view and dangerous in term of control robustness. In contrast, the present approach only tries to compensate dynamic effects responsible for the open-loop system's instability. More precisely, the main idea is to cancel the mode-coupling by a first control stage, so as to obtain a cascade of subsystems the transient of which is then easier to control. The considered Hultèn system defined by (2) can be viewed as two coupled dynamical subsystems (Σ_1 and Σ_2) where the dynamics of X_2 is affected by the dynamics of X_1 and vice-versa. This interpretation is represented in the upper diagram of Figure (4). The first step is to cancel the coupling effect (represented by the blue return loop in the upper diagram of Figure (4)) by using a control action. This is formalized by the following proposition.

Proposition 1 *Let*

$$u = m\left[\mu\left(w_1^2 X_1 + \psi_1^{NL} X_1^3\right) + \bar{u}(x)\right] \tag{6}$$

Then, when $\bar{u}(x) \equiv 0$, u applied to System (2) ensures the following properties:

1. *The dynamics of X_2 is independent of the dynamics of X_1.*
2. *The origin $x = 0$ is globally asymptotically stable (GAS).*

The first property of this proposition is easy to verify. Indeed, it follows from (2) and (6) with $\bar{u}(x) \equiv 0$ that:

$$\ddot{X}_2 = -w_2^2 X_2 - \eta_2 w_2 \dot{X}_2 - \psi_2^{\mathrm{NL}} X_2^3 \tag{7}$$

This shows that X_2's dynamics is now independent of the dynamics of X_1, i.e., the interaction between the subsystems Σ_1 and Σ_2 in Figure (4) is cancelled. The proof of the second property is provided in Appendix 1.

The previous control is very simple but it is not sufficient to ensure good transient characteristics. This control law can be easily modified to tune X_2's transient behavior. Indeed, by setting

$$\bar{u} = (\eta_2 - 2\xi_2)\, w_2 \dot{X}_2 \tag{8}$$

instead of $\bar{u} = 0$ one obtains in closed-loop:

$$\ddot{X}_2 = -w_2^2 X_2 - 2\xi_2 w_2 \dot{X}_2 - \psi_2^{\mathrm{NL}} X_2^3 \tag{9}$$

Choosing a suitable damping coefficient ξ_2 (e.g., $\xi_2 = \frac{1}{\sqrt{2}}$) ensures good damping of X_2's dynamics. With such a control law, however, X_1's dynamics will remain poorly damped. Hence, the next idea is to exploit the cascade structure depicted in Figure (4) (lower diagram), in which X_2 can be viewed as a virtual control input of the subsystem Σ_1 defining the dynamics of X_1. Then, this virtual control input can be exploited to tune the transient properties of X_1. This idea is formalized in the following proposition.

Proposition 2 *Let*

$$\tilde{X}_2 = X_2 + \tau \dot{X}_1 \,, \qquad \tau = \frac{w_1}{\mu w_2^2}(2\xi_1 - \eta_1) \tag{10}$$

where $\tilde{X}_2$ can be viewed as a tracking error and let

$$u = m\left[\mu\left(w_1^2 X_1 + \psi_1^{NL} X_1^3\right) + \psi_2^{NL} X_2^3 + \bar{u}(x)\right] \tag{11}$$

with

$$\bar{u}(x) = -\tau \dddot{X}_1 - \tau w_2^2 \dot{X}_1 + (\eta_2 - 2\xi_2) w_2 \dot{X}_2 - 2\tau \xi_2 w_2 \ddot{X}_1 \tag{12}$$

and $\xi_2 > 0$. Then, if $2\xi_1 > \eta_1$, u applied to System (2) ensures the following properties:

1. *The origin $x = 0$ is GAS.*
2. *The characteristic polynomial of the linearized closed-loop system is given by:*

$$Q(p) = (p^2 + 2\xi_1 w_1 p + w_1^2)(p^2 + 2\xi_2 w_2 p + w_2^2) \tag{13}$$

The proof of Proposition (2) is given in Appendix 2.

The above proposition provides guarantees about the global asymptotic stability of the closed loop system and the poles of the linearized closed-loop systems. Note that the open-loop natural frequencies of the linearized system are conserved in closed-loop, i.e., the control law only modifies the damping coefficients. Note also that the control expression (11) is similar to the control expression (6) modulo the term $\psi_2^{\mathrm{NL}} X_2^3$. As a matter of fact, one can verify that the conclusions of Proposition 1 also hold with the control law (11) when setting $\bar{u}(x) \equiv 0$. Choosing $\bar{u}(x)$ as in (12), however, is instrumental in order to improve X_1's transient dynamics. In this respect, the control law of Proposition 2 is designed so that $\tilde{X}_2$ converges asymptotically to zero. Hence X_2 approaches asymptotically $-\tau \dot{X}_1$, which explains the role of X_2 in providing additional damping for X_1's dynamics.

Figure (5) reports simulation results obtained with the control laws (3) and (11). It can be observed from Figure (5)-(a,b) that the transient of the displacement X_1 obtained with the control law (11) is rapidly and strongly damped compared to the one obtained by using (3), thus leading to a much smaller settling time. The control amplitudes are still important but by comparing Figure(5)-(c,d). and Figure (3)-(f), one can observe that the control amplitude with the control law (11) is much lower than the control amplitude observed with the control law (3)-(4) obtained by feedback linearization, despite the fact that the settling time and transient dynamics of the former is much better than those of the latter. This illustrates the significant improvement achieved with this new controller.

Another interesting comparison aspect concerns the control sensitivity to control saturation. In practice, high amplitude controls may lead to actuators saturation phenomena, which potentially deteriorate the closed-loop system's performance. This issue is illustrated in the following via simulation results obtained with the control (11). To this goal, the control input (11) is saturated at a maximum amplitude of ± 100 Vlt. Note that this is a drastic saturation value compared to the maximum value reached by the non-saturated control. The control saturation effect is clearly visible on Figure (6)-(a). The corresponding controlled displacement X_1 is displayed on Figures (6)-(b,c) together with the one obtained from the non-saturated version of the control law (11). The results clearly show that the performances of the closed-loop system are impacted by the saturation, as shown by the induced vibrations with relatively high amplitudes. However, convergence to zero of X_1 is still achieved with a decent settling time despite the drastic saturation level. This robustness with respect to the control saturation was not observed with the feedback linearizing control (3)-(4): in simulation results not reported in this paper for sake of brevity, it was observed with that controller that with the same level of control saturation X_1 did not converge to zero asymptotically anymore. Robustness to control saturation is another asset of the control solution proposed in this paper.

Finally and in order to complete the robustness analysis of the proposed controller, parameter uncertainty is considered. In fact, FIV are known to be submitted to parameter uncertainty. The friction coefficient is one of the most influential parameters on FIV ([20, 10, 18, 57, 44, 37]. Furthermore, this parameter is submitted to dispersion. Hence, in practice, the controller of FIV is required to be robust with respect to parameter uncertainty and more particularly to that of the friction coefficient. Hence, the controlled Hultèn system is simulated for different values of the friction coefficient within the interval $[0.38, 0.42]$. Results are shown in Figure (7). The linearizing state feedback given by (3) and (4) and the new proposed controller defined by (11) and (12) are considered. Deviations of the friction coefficient

around its nominal value destabilize the closed-loop system based on the linearizing state feedback. The latter is clearly not robust with respect to the considered uncertainty. Unlike the linearizing state feedback, the controller (11) and (12) exhibits a suitable robustness since the asymptotic stability is kept and the transient regime is only weakly impacted.

4 Control of a Hoffman-like friction system

In this subsection, another mechanical system (8) submitted to mode-coupling instabilities but with a higher number of degrees of freedom is considered. The main aim is to analyse the proposed transient control method when used for mitigating mode-coupling based FIV in more complex systems. The system, which is a Hoffman-like friction system used for modelling and controlling mode-coupling instabilities [45, 11], is a slider-belt consisting of three masses $m_{i\in\{1,2,3\}}$. Only the mass m_2 possesses degrees of freedom in the horizontal and vertical directions while m_1 and m_3 have a d.o.f in the horizontal and vertical directions respectively. The belt is supposed to move with a constant velocity while a pre-compression normal force is also considered at the slider-belt interface. The Coulomb law with a constant friction coefficient μ is considered as that governing the friction at the slider-belt interface. The dynamical behaviour of the system is then governed by a System (1)-like differential equation with:

$$\mathrm{M}=\begin{bmatrix} m_1 & 0 & 0 & 0\\ 0 & m_3 & 0 & 0\\ 0 & 0 & m_2 & 0\\ 0 & 0 & 0 & m_2 \end{bmatrix},\ \mathrm{K}=\begin{bmatrix} k_1+k_2 & 0 & -k_2 & 0\\ 0 & k_4+k_5 & 0 & -k_4\\ -k_2 & 0 & k_2+0.5k_3 & -0.5k_3+\mu k_c\\ 0 & -k_4 & -0.5k_3 & k_4+0.5k_3+k_c \end{bmatrix} \tag{14}$$

$$\mathrm{C}=\begin{bmatrix} c_1 & 0 & -c_1 & 0\\ 0 & 0 & 0 & 0\\ -c_1 & 0 & c_1 & 0\\ 0 & 0 & 0 & c_0 \end{bmatrix},\ \mathrm{F_{NL}(X)}=\begin{bmatrix} 0\\ 0\\ k_{nl}x_2^3\\ 0 \end{bmatrix},\ \text{and } X=\begin{bmatrix} x_1\\ y_3\\ x_2\\ y_2 \end{bmatrix} \tag{15}$$

For numerical application, all values are given in SI, with $m_1=1$, $m_2=0.5$, $m_3=1$, $c_0=0.2$, $c_1=0.1$, $k_1=5$, $k_2=25$,$k_3=25$, $k_4=0.05$, $k_5=0.05$, $k_c=10k_1$ and $k_{c_{nl}}=1000k_1$.

By performing the stability analysis against the friction coefficient μ, based on the indirect Lyapunov method, the mode-coupling phenomenon can be observed with a mode-coalescence occurring at $\mu_c=0.2538$. The system presents unstable behaviour with limit cycle oscillations as shown in Figure (10)-(a,b) where the displacements x_1 and y_3 are plotted. These vibrations are required to be suppressed while ensuring suitable transient properties.

Applying the method proposed for the Hultèn system to the present system, so as to obtain the cascade configuration given in Figure (9)-(c) from structures in Figure (9)-(a) and (b) respectively, requires two control inputs. We assume that the system is endowed with two control inputs, which correspond to a control force on the mass m_2 in both the horizontal and vertical direction. The matrix B in (1) is thus given by

$$B=\begin{bmatrix} 0 & 0\\ 0 & 0\\ 1 & 0\\ 0 & 1 \end{bmatrix} \tag{16}$$

Mimicking Proposition 1, we first define a change of control input variables that removes the coupling loop between Σ_2 and Σ_3 (See Figure (9)-(a)):

$$\left\{\begin{array}{lcl} u_1 &=& (\mu k_c-0.5k_3)y_2+\bar{u}_1\\ u_2 &=& -0.5k_3x_2+\bar{u}_2 \end{array}\right. \tag{17}$$

Then, one obtains two virtual independent subsystems namely (Σ_1,Σ_2) and (Σ_3,Σ_4), the structure of which is similar to the Hultèn system given in Figure (4). These two subsystems are represented on Figure (9)-(b). One can then apply to each of these subsystems the approach of Section 3, i.e. decoupling (Proposition 1) as shown on Figure (9)-(c), and transient tuning (Proposition 2), with x_2 and y_2 viewed as virtual control inputs for the subsystems Σ_1 and Σ_4 respectively. Finally, we obtain the following result, the proof of which is given in the Appendix.

Proposition 3 *Consider damping coefficients $\xi_1, \cdots, \xi_4 > 0$ and assume that:*

$$\xi_1 \geq \frac{c_1}{2\sqrt{m_1(k_1+k_2)}} \tag{18}$$

Let

$$\bar{u}_1 = -m_2(\tau_1\varpi_2^2\dot{x}_1 + \tau_1\dddot{x}_1) - \left(c_1(\dot{x}_1 - \dot{x}_2) + k_2x_1 - k_{nl}x_2^3\right) - 2m_2\xi_2\varpi_2\dot{\tilde{x}}_2 \tag{19}$$

with

$$\tau_1 = \frac{c_1(2\xi_1^2\varpi_1^2m_1 - k_2) + \sqrt{c_1^2(k_2 - 2\xi_1^2\varpi_1^2m_1)^2 + k_2^2(4\xi_1^2m_1(k_1+k_2) - c_1^2)}}{k_2^2} \tag{20}$$

$$\varpi_2 = \sqrt{\frac{k_2 + 0.5k_3}{m_2}}$$

and $\tilde{x}_2 = x_2 + \tau_1\dot{x}_1$, and let

$$\bar{u}_2 = -\left[c_0\tau_2\ddot{y}_3 + m_2\varpi_3^2\tau_2\dot{y}_3 + k_4y_3\right] + (c_0 - 2m_2\xi_3\varpi_3)\,\dot{\tilde{y}}_2 \tag{21}$$

with

$$\tau_2 = \frac{2m_3\xi_4\varpi_4}{k_4}\,, \quad \varpi_3 = \sqrt{\frac{k_4 + 0.5k_3 + k_c}{m_2}}\,, \quad \varpi_4 = \sqrt{\frac{k_4+k_5}{m_3}}$$

and $\tilde{y}_2 = y_2 + \tau_2\dot{y}_3$.

Then, the origin of the closed-loop system is globally asymptotically stable.

This proposition calls for several remarks:

1. Another control solution with a slightly simpler control expression can be proposed. More precisely, in the change of control variable (17) the second change of control variable is not necessary. Indeed, if we simply let $u_2 = \bar{u}_2$, the subsystems (Σ_1, Σ_2) and (Σ_3, Σ_4) will no longer be independent but they will be in cascade form, i.e., (Σ_1, Σ_2) will affect (Σ_3, Σ_4) but the converse will not be true. This breaking of the coupling loop is sufficient to ensure GAS and good transient properties, with $\bar{u}_1$ and $\bar{u}_2$ still defined as in Proposition 3.
2. The new variables $\tilde{x}_2$ and $\tilde{y}_2$ used in the definition of $\bar{u}_1$ and $\bar{u}_2$ respectively play the same role as the new variable $\tilde{X}_2$ in (10). They allow one to provide additional damping for the variables x_1 and y_3 respectively.
3. The control parameters $\xi_1, \cdots, \xi_4 > 0$ are user-defined damping coefficients used to tune the damping for the variables x_1, x_2, y_2, and y_3 respectively (see the proof of the proposition in the appendix for details). Thus, typical values of these coefficients should be around $1/\sqrt{2}$.

Then, by applying both control laws u_1 and u_2 given by (17) with (19) and (21), the system is asymptotically stabilized as predicted and stated in Proposition 3. Indeed, the observed oscillations on Figure (10) are suppressed. The properties of the corresponding transients depend on the damping rates ξ_1, ξ_2, ξ_3 and ξ_4. Since the subsystems (Σ_1, Σ_2) and (Σ_1, Σ_2) are independent, then, the corresponding transients properties can be controlled separately by tuning the couples of damping rates (ξ_1, ξ_2) and (ξ_3, ξ_4) respectively. The systems displacements x_1 and y_3 corresponding to the damping rates equal to 0.3, 0.5 and 0.7 are plotted in Figure (11). The corresponding control laws u_1 and u_2 are also plotted in Figure (12). The well known effect of the damping is observed. Indeed, the amplitude of the mitigated vibrations and thus the settling times decrease when augmenting the damping rates. Otherwise, the counterpart of these effects is essentially related to the control amplitudes. The higher the damping rate, the greater the amplitudes of the control signal. A compromise is necessary in practice, all the more so since high amplitudes for the control can, as mentioned previously in the first example, lead to saturation phenomena, the effects of which can be very detrimental to performances. In this framework and as in the previous subsection, we propose here to evaluate the robustness of the cascade structure based control with respect to the control saturation. The main idea is to evaluate the sensibility of the control strategy toward the occurrence of the saturation phenomenon. The control signals u_1 and u_2 are saturated to maximal values equal to ± 0.01 Volt. The corresponding displacements x_1 and y_3 are shown in Figure (14) while the non-saturated and saturated controls u_1 and u_2 are plotted in Figure (13). These results are obtained with the damping rates fixed to 0.7.

The performances of the closed loop system have been slightly impacted. In particular the introduced

non-linearities (saturations) have induced greater amplitudes in the transients of the two considered displacements x_1 and y_3 but without consequences on the asymptotic stability of the closed loop system equilibrium. The results show that given the severe level of saturation brought to the controls, the sensitivity of the performances is quite low, which confirms the results of the previous section for the Hultèn system.

As for the Hultèn system and in the same way, the robustness to parameter uncertainty of the controller defined by (17), (19), and (21) is analyzed. Friction coefficient variations are also considered, within the interval $[0.45, 0.55]$, which corresponds to a high uncertainty compared to the one often considered in practice (in general it does not exceed 5% around the nominal value).
The controlled displacements x_1 and y_3 are plotted in Figure (15)-(a,b,c,d) for $\mu = 0.45$ and $\mu = 0.55$. The asymptotic stability of the controlled system is not perturbed by the considered uncertainty. The corresponding transients are also not impacted which, as previously observed with the Hultèn system, indicates the robustness of the controller with respect to the considered uncertainty.

5 Conclusion

This study has shown the great benefits to use a new control technique for mitigating Friction-induced Vibration occasioned by the mode-coupling mechanism. The presented technique considers a preliminary control stage in order to put the friction system into a cascade of sub-systems. Each subsystem can then be controlled more efficiently. In particular, properties of the transient regime prove to be easier to efficiently control. Moreover, interesting robustness properties with respect to the saturation phenomenon and parameter uncertainty have been numerically shown for the proposed control scheme.

The efficiency of the proposed cascade architecture based control was assessed by considering minimal models submitted to mode-coupling instabilities. The obtained results are convincing, which gives promising perspectives in terms of the capacities of the proposed control scheme to be considered and extended for real world applications.

Appendix 1: **Proof of Proposition 1:** As mentioned after the statement of Proposition 1, Property 1 is easily verified. Therefore, we focus on Property 2. Consider the candidate Lyapunov function for System (7):

$$V_2(X_2, \dot{X}_2) := \frac{1}{4}\left(2w_2^2X_2^2 + 2\dot{X}_2^2 + 4\alpha_2 X_2\dot{X}_2 + \psi_2^{\mathrm{NL}}X_2^4\right) \tag{22}$$

with

$$\alpha_2 := \min\left(\frac{w_2}{2}, \frac{2\eta_2 w_2}{4+\eta_2^2}\right) \tag{23}$$

Since $0 < \alpha_2 < w_2$, $2w_2^2X_2^2 + 2\dot{X}_2^2 + 4\alpha_2 X_2\dot{X}_2$ defines a positive-definite quadratic form of $X_2, \dot{X}_2$ and thus $V_2(X_2, \dot{X}_2) > 0$ for $(X_2, \dot{X}_2) \neq (0, 0)$. The time-derivative of V_2 along the solutions of System (7) is given by

$$\dot{V}_2(X_2, \dot{X}_2) = -\alpha_2 w_2^2 X_2^2 - \alpha_2\eta_2\omega_2 X_2\dot{X}_2 - (\eta_2 w_2 - \alpha_2)\dot{X}_2^2 - \alpha_2\psi_2^{\mathrm{NL}}X_2^4$$

Eq. (23) implies that $0 < \alpha_2 < \frac{4\eta_2 w_2}{4+\eta_2^2}$, so that $\alpha_2 w_2^2 X_2^2 + \alpha_2\eta_2\omega_2 X_2\dot{X}_2 + (\eta_2 w_2 - \alpha_2)\dot{X}_2^2$ defines a positive-definite quadratic form of $X_2, \dot{X}_2$. This implies that $\dot{V}(X_2, \dot{X}_2) < 0$ for $(X_2, \dot{X}_2) \neq (0, 0)$. More precisely, there exists a constant scalar $c > 0$ such that

$$\dot{V}_2(X_2, \dot{X}_2) \leq -c\left(X_2^2 + \dot{X}_2^2 + X_2^4\right) \tag{24}$$

Let us now consider the candidate Lyapunov function for the complete controlled system, i.e., (2)-(6):

$$V(x) = V_1(X_1, \dot{X}_1) + \beta\left(V_2(X_2, \dot{X}_2) + V_2^2(X_2, \dot{X}_2)\right)$$

with

$$V_1(X_1, \dot{X}_1) := \frac{1}{4}\left(2w_1^2X_1^2 + 2\dot{X}_1^2 + \psi_1^{\mathrm{NL}}X_1^4\right) \tag{25}$$

V_2 defined by (22), and $\beta > 0$ a constant scalar parameter. From (2), the time-derivative of V_1 along the solutions of the controlled system is given by

$$\dot{V}_1(X_1, \dot{X}_1) = -\eta_1 w_1 \dot{X}_1^2 + \mu \dot{X}_1 \left(w_2^2 X_2 + \psi_2^{\mathrm{NL}} X_2^3 \right)$$

Thus, the time-derivative of V along the solutions of the controlled system is given by

$$\begin{aligned} \dot{V}(x) &= \dot{V}_1(X_1, \dot{X}_1) + \beta \left(1 + 2V_2(X_2, \dot{X}_2) \right) \dot{V}_2(X_2, \dot{X}_2) \\ &\leq -\eta_1 w_1 \dot{X}_1^2 + \mu \dot{X}_1 \left(w_2^2 X_2 + \psi_2^{\mathrm{NL}} X_2^3 \right) \dots \\ &- c\beta \left(1 + 2V_2(X_2, \dot{X}_2) \right) \left(X_2^2 + \dot{X}_2^2 + X_2^4 \right) \\ &\leq -\eta_1 w_1 \dot{X}_1^2 + \mu \dot{X}_1 \left(w_2^2 X_2 + \psi_2^{\mathrm{NL}} X_2^3 \right) - c\beta \left(X_2^2 + \dot{X}_2^2 + \frac{w_2^2}{2} X_2^6 \right) \end{aligned} \tag{26}$$

where the last equation comes from the fact that $V_2(X_2, \dot{X}_2) \geq \frac{w_2^2}{4} X_2^2$ because, in view of (23),

$$w_2^2 X_2^2 + 2\dot{X}_2^2 + 4\alpha_2 X_2 \dot{X}_2$$

is a positive quadratic form of $X_2, \dot{X}_2$. Then, by using the triangular inequality, one verifies from (26) that $\dot{V}(x)$ is upper-bounded by a negative-definite quadratic function of $\dot{X}_1, X_2, X_2^3$, and $\dot{X}_2$ provided that β is chosen large enough. This shows that V is a non-strict Lyapunov function for the controlled system. By application of the LaSalle invariance principe (see, e.g., [34, Pg. 128], all trajectories converge towards the largest invariant set contained in $E = \{x : \dot{V}(x) = 0\} = \{x : \dot{X}_1 = X_2 = \dot{X}_2 = 0\}$. Any solution $x(t)$ of the controlled system contained in E for all times satisfies $\dot{X}_1(t) = X_2(t) = \dot{X}_2(t) = 0\,,\ \forall t$ and thus, $\ddot{X}_1(t) = \dot{X}_1(t) = X_2(t) = \dot{X}_2(t) = 0\,,\ \forall t$. This implies, from the first equation in (2), that $X_1(t) = 0$ for all t, and thus $x(t) = 0\,,\ \forall t$. Thus, the largest invariant set for the system contained in E is reduced to the origin and all solutions converge to the origin. Since V is a Lyapunov function, stability is also granted, which concludes the proof.

∎

Appendix 2: **Proof of Proposition 2:** From the definition of $\tilde{X}_2$,

$$\begin{aligned} \dddot{\tilde{X}}_2 &= \ddot{X}_2 + \tau \dddot{X}_1 \\ &= -w_2^2 X_2 - \eta_2 w_2 \dot{X}_2 + \bar{u}(x) + \tau \dddot{X}_1 \\ &= -w_2^2 \tilde{X}_2 - 2\xi_2 w_2 \ddot{\tilde{X}}_2 \end{aligned} \tag{27}$$

The dynamics of X_1 can be rewritten as follows:

$$\begin{aligned} \ddot{X}_1 &= -w_1^2 X_1 - \eta_1 w_1 \dot{X}_1 + \mu w_2^2 X_2 - \psi_1^{\mathrm{NL}} X_1^3 + \mu \psi_2^{\mathrm{NL}} X_2^3 \\ &= -w_1^2 X_1 - \eta_1 w_1 \dot{X}_1 + \mu w_2^2 (\tilde{X}_2 - \tau \dot{X}_1) - \psi_1^{\mathrm{NL}} X_1^3 + \mu \psi_2^{\mathrm{NL}} (\tilde{X}_2 - \tau \dot{X}_1)^3 \\ &= -w_1^2 X_1 - (\eta_1 w_1 + \mu \tau w_2^2) \dot{X}_1 - \psi_1^{\mathrm{NL}} X_1^3 - \mu \psi_2^{\mathrm{NL}} \tau^3 \dot{X}_1^3 \\ &\quad + \mu w_2^2 \tilde{X}_2 + \mu \psi_2^{\mathrm{NL}} \tilde{X}_2 \left(\tilde{X}_2^2 - 3\tau \tilde{X}_2 \dot{X}_1 + 3\tau^2 \dot{X}_1^2 \right) \\ &= -w_1^2 X_1 - (\eta_1 w_1 + \mu \tau w_2^2) \dot{X}_1 - \psi_1^{\mathrm{NL}} X_1^3 - \mu \psi_2^{\mathrm{NL}} \tau^3 \dot{X}_1^3 + \mu \tilde{X}_2 h(\tilde{X}_2, \dot{X}_1) \\ &= -w_1^2 X_1 - 2\xi_1 w_1 \dot{X}_1 - \psi_1^{\mathrm{NL}} X_1^3 - \mu \psi_2^{\mathrm{NL}} \tau^3 \dot{X}_1^3 + \mu \tilde{X}_2 h(\tilde{X}_2, \dot{X}_1) \end{aligned} \tag{28}$$

with

$$h(\tilde{X}_2, \dot{X}_1) := w_2^2 + \psi_2^{\mathrm{NL}} \left(\tilde{X}_2^2 - 3\tau \tilde{X}_2 \dot{X}_1 + 3\tau^2 \dot{X}_1^2 \right) \tag{29}$$

Let us first establish Property 1 of Proposition 2. To this purpose, we will build a Lyapunov function. Since ω_2 and ξ_2 are strictly positive, Eq. (27) defines an asymptotically stable second-order linear system. Thus, by Lyapounov's theorem (see, e.g., [34, Th. 4.6], for any symmetric positive-definite matrix Q, there exists a symmetric positive-definite matrix P satisfying the Lyapunov equation, i.e.,

$$PA + A^T P + Q = 0$$

with

$$A = \begin{pmatrix} 0 & 1 \\ -w_2^2 & -2\xi_2 w_2 \end{pmatrix}$$

the state-space matrix associated with System (27). Let us for example set $Q = I_2$ with I_2 the 2×2 identity matrix. Then, the time-derivative, along the solutions to this system, of the Lyapounov candidate function

$$V_2(\tilde{X}_2, \dot{\tilde{X}}_2) := (\tilde{X}_2, \dot{\tilde{X}}_2) P (\tilde{X}_2, \dot{\tilde{X}}_2)^T \tag{30}$$

satisfies the equation

$$\dot{V}_2(X_2, \dot{\tilde{X}}_2) = -\left(\tilde{X}_2^2 + \dot{\tilde{X}}_2^2\right) \tag{31}$$

Let us now define a function V_1 by the relation

$$V_1(X_1, \dot{X}_1) = w_1^2 \frac{X_1^2}{2} + \psi_1^{\rm NL} \frac{X_1^4}{4} + \frac{\dot{X}_1^2}{2}$$

From (28), the time-derivative of V_1 along the solutions of the system is given by

$$\begin{array}{rcl} \dot{V}_1(X_1, \dot{X}_1) & = & w_1^2 X_1 \dot{X}_1 + \psi_1^{\rm NL} X_1^3 \dot{X}_1 + ... \\ & & \dot{X}_1 \left(-w_1^2 X_1 - 2\xi_1 w_1 \dot{X}_1 - \psi_1^{\rm NL} X_1^3 - \mu \psi_2^{\rm NL} \tau^3 \dot{X}_1^3 + \mu \tilde{X}_2 h(\tilde{X}_2, \dot{X}_1) \right) \\ & = & -2\xi_1 \omega_1 \dot{X}_1^2 - \mu \tau^3 \psi_2^{\rm NL} \dot{X}_1^4 + \mu \tilde{X}_2 \dot{X}_1 h(\tilde{X}_2, \dot{X}_1) \end{array} \tag{32}$$

Note that $\tau > 0$, due to (10) and the Proposition's assumption that $2\xi_1 > \eta_1$. Thus, both terms $-2\xi_1\omega_1\dot{X}_1^2$ and $-\mu\tau^3\psi_2^{\rm NL}\dot{X}_1^4$ in the expression of $\dot{V}_1$ are negative. We claim that the function

$$V(x) := V_1(X_1, \dot{X}_1) + \lambda V_2(\tilde{X}_2, \dot{\tilde{X}}_2)(1 + V_2(\tilde{X}_2, \dot{\tilde{X}}_2))$$

is a (non-strict) Lyapunov function for the system provided that $\lambda > 0$ is chosen large enough. From (31) and (32), we have

$$\begin{array}{rcl} \dot{V}(x) & = & \dot{V}_1(X_1, \dot{X}_1) + \lambda \dot{V}_2(\tilde{X}_2, \dot{\tilde{X}}_2)(1 + 2V_2(\tilde{X}_2, \dot{\tilde{X}}_2)) \\ & = & -2\xi_1\omega_1\dot{X}_1^2 - \mu\tau^3\psi_2^{\rm NL}\dot{X}_1^4 - \lambda\left(\tilde{X}_2^2 + \dot{\tilde{X}}_2^2\right)(1 + 2V_2(\tilde{X}_2, \dot{\tilde{X}}_2)) \\ & & +\mu\tilde{X}_2\dot{X}_1 h(\tilde{X}_2, \dot{X}_1) \end{array} \tag{33}$$

Let us consider the term $\mu\tilde{X}_2\dot{X}_1 h(\tilde{X}_2, \dot{X}_1)$ in the last line of the above equation. From (29),

$$\mu\tilde{X}_2\dot{X}_1 h(\tilde{X}_2, \dot{X}_1) = \mu w_2^2 \tilde{X}_2 \dot{X}_1 + \mu\psi_2^{\rm NL}\tilde{X}_2^3\dot{X}_1 - 3\mu\tau\psi_2^{\rm NL}\tilde{X}_2^2\dot{X}_1^2 + 3\mu\tau^2\psi_2^{\rm NL}\tilde{X}_2\dot{X}_1^3 \tag{34}$$

We recall the Holder inequality:

$$ab \le \frac{1}{p}a^p + \frac{1}{q}b^q$$

with $a, b \ge 0$, $p, q > 0$, and $\frac{1}{p} + \frac{1}{q} = 1$. We first apply this inequality with $p = q = 2$ (i.e., the usual triangular inequality) to the first term in (34):

$$\mu w_2^2 \tilde{X}_2\dot{X}_1 \le |\mu w_2^2 \tilde{X}_2\dot{X}_1| \le 2\xi_1 w_1 \frac{\mu w_2^2}{2\xi_1 w_1}|\tilde{X}_2||\dot{X}_1| \le \xi_1 w_1 \left[\left(\frac{\mu w_2^2}{2\xi_1 w_1}\right)^2 \tilde{X}_2^2 + \dot{X}_1^2\right] \tag{35}$$

We now apply the Holder inequality with $p = 4$ and $q = \frac{4}{3}$ to the second and last terms in (34):

$$\mu\psi_2^{\rm NL}\tilde{X}_2^3\dot{X}_1 \le |\mu\psi_2^{\rm NL}\tilde{X}_2^3\dot{X}_1| \le \mu\tau^3\psi_2^{\rm NL}\frac{1}{\tau^3}|\tilde{X}_2^3||\dot{X}_1| \le \frac{\mu\tau^3\psi_2^{\rm NL}}{4}\left[\frac{3}{\tau^4}\tilde{X}_2^4 + \dot{X}_1^4\right] \tag{36}$$

$$\begin{array}{rcl} 3\mu\tau^2\psi_2^{\rm NL}\tilde{X}_2\dot{X}_1^3 \le |3\mu\tau^2\psi_2^{\rm NL}\tilde{X}_2\dot{X}_1^3| \le \frac{\mu\tau^3\psi_2^{\rm NL}}{3}\frac{9}{\tau}|\tilde{X}_2||\dot{X}_1^3| \dots \\ \le \frac{\mu\tau^3\psi_2^{\rm NL}}{4}\left[\frac{9^4}{3\tau^4}\tilde{X}_2^4 + \dot{X}_1^4\right] \end{array} \tag{37}$$

Noting that the third term in the right-hand side of (34) is negative, we deduce from (34)–(37) that

$$\begin{array}{rcl}\mu\tilde{X}_2\dot{X}_1h(\tilde{X}_2,\dot{X}_1) & \leq & \tilde{X}_2^2\left(\xi_1w_1\left(\frac{\mu w_2^2}{2\xi_1w_1}\right)^2\right)\\ & & +\tilde{X}_2^4\left(\frac{\mu\tau^3\psi_2^{\rm NL}}{4}\left(\frac{3}{\tau^4}+\frac{9^4}{3\tau^4}\right)\right)\\ & & +\dot{X}_1^2\left(\xi_1w_1\right)\\ & & +\dot{X}_1^4\left(\frac{\mu\tau^3\psi_2^{\rm NL}}{2}\right)\end{array} \tag{38}$$

We deduce from (33) and (38) that

$$\begin{array}{rcl}\dot{V}(x) & \leq & -\xi_1w_1\dot{X}_1^2-\frac{\mu\tau^3\psi_2^{\rm NL}}{2}\dot{X}_1^4\\ & & -\tilde{X}_2^2\left[\lambda(1+2V_2(\tilde{X}_2,\dot{\tilde{X}}_2))-\xi_1w_1\left(\frac{\mu w_2^2}{2\xi_1w_1}\right)^2\right]\\ & & +\tilde{X}_2^4\left(\frac{\mu\tau^3\psi_2^{\rm NL}}{4}\left(\frac{3}{\tau^4}+\frac{9^4}{3\tau^4}\right)\right)\\ & & -\lambda\dot{\tilde{X}}_2^2\left(1+2V_2(\tilde{X}_2,\dot{\tilde{X}}_2)\right)\end{array} \tag{39}$$

Since V_2 is a positive definite quadratic form of $\tilde{X}_2$ and $\dot{\tilde{X}}_2$, there exists a constant scalar $c>0$ such that $V_2(\tilde{X}_2,\dot{\tilde{X}}_2)\geq c\tilde{X}_2^2$. Thus, we deduce from the above inequality that

$$\begin{array}{rcl}\dot{V}(x) & \leq & -\xi_1w_1\dot{X}_1^2-\frac{\mu\tau^3\psi_2^{\rm NL}}{2}\dot{X}_1^4\\ & & -\tilde{X}_2^2\left[\lambda-\xi_1w_1\left(\frac{\mu w_2^2}{2\xi_1w_1}\right)^2\right]\\ & & -\tilde{X}_2^4\left(2\lambda c-\frac{\mu\tau^3\psi_2^{\rm NL}}{4}\left(\frac{3}{\tau^4}+\frac{9^4}{3\tau^4}\right)\right)\\ & & -\lambda\dot{\tilde{X}}_2^2\left(1+2V_2(\tilde{X}_2,\dot{\tilde{X}}_2)\right)\end{array} \tag{40}$$

It follows from the above inequality that $\dot{V}(x)\leq 0$ for all x provided that λ is chosen large enough. V is not a strict Lyapounov function, however, since the set where $\dot{V}(x)=0$ is not reduced to $\{0\}$. To conclude to the GAS property, we make use of the LaSalle theorem and its application proceeds exactly like in the proof of Proposition 1 to show that all trajectories converge to the origin $x=0$.

We now establish the second property of Proposition 2. To this purpose, for any time-function z, we denote by $[z](p)$ the Laplace transform of z. Let us recall that for a mono-input linear system $\dot{x}=Ax+bu$, the polynomial characteristic of A corresponds to the common denominator of the transfer functions between u and the x_i's. Assume that the control $u+m\delta u$ is applied to System (2) with u given by (11). Then, Equation (27) becomes

$$\ddot{\tilde{X}}_2=-w_2^2\tilde{X}_2-2\xi_2w_2\dot{\tilde{X}}_2+\delta u \tag{41}$$

Applying the Laplace transform to this equation (with null initial conditions) gives:

$$(p^2+2\xi_2w_2p+w_2^2)[\tilde{X}_2](p)=[\delta u](p)$$

Since $\tilde{X}_2=X_2+\tau\dot{X}_1$, this equation yields:

$$(p^2+2\xi_2w_2p+w_2^2)([X_2](p)+\tau p[X_1](p))=[\delta u](p) \tag{42}$$

Then, it follows from the first equality in (28), after neglecting nonlinear terms, that the linearized dynamics of X_1 satisfies the following equation:

$$\ddot{X}_1=-w_1^2X_1-\eta_1w_1\dot{X}_1+\mu w_2^2X_2 \tag{43}$$

Applying the Laplace transform to this equation gives:

$$(p^2+\eta_1w_1p+w_1^2)[X_1](p)=\mu w_2^2[X_2](p)$$

Replacing the expression of $[X_2](p)$ given by this equation in (42) yields:

$$(p^2+2\xi_2w_2p+w_2^2)\left(\frac{p^2+\eta_1w_1p+w_1^2}{\mu w_2^2}[X_1](p)+\tau p[X_1](p)\right)=[\delta u](p)$$

By using the expression of τ given by (10), we obtain:

$$(p^2 + 2\xi_2 w_2 p + w_2^2)\left(\frac{p^2 + 2\xi_1 w_1 p + w_1^2}{\mu w_2^2}\right)[X_1](p) = [\delta u](p)$$

so that:

$$[X_1](p) = \frac{\mu w_2^2}{(p^2 + 2\xi_2 w_2 p + w_2^2)(p^2 + 2\xi_1 w_1 p + w_1^2)}[\delta u](p)$$

Thus, $Q(p)$ as defined by (13) is the denominator of the transfer function from δu to X_1. Since this is a fourth-order polynomial, it corresponds to the characteristic polynomial of the linearized closed-loop system. ∎

Appendix 3: **Proof of Proposition 3:** By applying the change of control input (17), one verifies from (14), (15), and (16) that the following two independent subsystems are obtained:

$$\left\{\begin{array}{lcl} m_1\ddot{x}_1 &=& -c_1\dot{x}_1 + c_1\dot{x}_2 - (k_1+k_2)x_1 + k_2x_2 \\ m_2\ddot{x}_2 &=& c_1\dot{x}_1 - c_1\dot{x}_2 + k_2x_1 - (k_2+0.5k_3)x_2 - k_{nl}x_2^3 + \bar{u}_1 \end{array}\right. \tag{44}$$

and

$$\left\{\begin{array}{lcl} m_2\ddot{y}_2 &=& -c_0\dot{y}_2 - (k_4+0.5k_3+k_c)y_2 + k_4y_3 + \bar{u}_2 \\ m_3\ddot{y}_3 &=& -(k_4+k_5)y_3 + k_4y_2 \end{array}\right. \tag{45}$$

We first consider Subsystem (45). This is a controllable linear system and thus any linear control method (pole placement, LQR, etc) could be used to make this system asymptotically stable. The proposed control expression $\bar{u}_2$ in (21) follows the cascade approach used for the Hultèn system, where y_2 is used to provide damping to the dynamics of y_3, via the new variable $\tilde{y}_2 = y_2 + \tau_2\dot{y}_3$. The advantage of this approach is that the natural frequency of the system is conserved in closed loop (i.e., only damping is modified). More precisely, one verifies from (21) and (45) that the closed-loop system can be rewritten, using $\tilde{y}_2$ in place of y_2, as follows:

$$\left\{\begin{array}{lcl} \dddot{\tilde{y}}_2 &=& -2\xi_3\varpi_3\ddot{\tilde{y}}_2 - \varpi_3^2\dot{\tilde{y}}_2 \\ \ddot{y}_3 &=& -2\xi_4\varpi_4\dot{y}_3 - \varpi_4^2 y_3 + \frac{k_4}{m_3}\tilde{y}_2 \end{array}\right.$$

Since $\xi_3, \varpi_3 > 0$, $\tilde{y}_2(t)$ converges exponentially to zero as $t \longrightarrow +\infty$, and on the zero-dynamics $\tilde{y}_2 \equiv 0$. The dynamics of y_3, defined by its natural frequency $\varpi_4 > 0$ and damping coefficient $\xi_4 > 0$, is also asymptotically stable. Asymptotic stability of Subsystem (45) is then straightforward.

We now consider Subsystem (44). Due to the term $k_{nl}x_2^3$ in the expression of $\ddot{x}_2$, this system is nonlinear. However, this nonlinearity can be easily cancelled with the control action $\bar{u}_1$. Then, the system becomes linear and it can be controlled with classical linear techniques. We also exploit the cascade approach for the gain tuning but its application is more tricky here because both x_2 and $\dot{x}_2$ affect the dynamics of x_1 in (44). Let $\tilde{x}_2 = x_2 + \tau_1\dot{x}_1$. One verifies from (19) and (44) that the closed-loop system can be rewritten, using $\tilde{x}_2$ in place of x_2, as follows:

$$\left\{\begin{array}{lcl} \ddot{x}_1 &=& -\frac{c_1}{m_1}\dot{x}_1 + \frac{c_1}{m_1}(\dot{\tilde{x}}_2 - \tau_1\ddot{x}_1) - \varpi_1^2 x_1 + \frac{k_2}{m_1}(\tilde{x}_2 - \tau_1\dot{x}_1) \\ \ddot{\tilde{x}}_2 &=& -2\xi_2\varpi_2\dot{\tilde{x}}_2 - \varpi_2^2\tilde{x}_2 \end{array}\right.$$

with

$$\varpi_1 = \sqrt{\frac{k_1+k_2}{m_1}}$$

Since $\xi_2, \varpi_2 > 0$, $\tilde{x}_2(t)$ converges exponentially to zero as $t \longrightarrow +\infty$, and on the zero-dynamics $\tilde{x}_2 \equiv 0$ while the dynamics of x_1 is defined by the following equation:

$$\ddot{x}_1 = -\frac{c_1}{m_1}\dot{x}_1 - \frac{c_1}{m_1}\tau_1\ddot{x}_1 - \varpi_1^2 x_1 - \frac{k_2}{m_1}\tau_1\dot{x}_1$$

This equation can be rewritten as follows:

$$\ddot{x}_1 = -\frac{c_1 + k_2\tau_1}{m_1 + c_1\tau_1}\dot{x}_1 - \frac{m_1\varpi_1^2}{m_1 + c_1\tau_1}x_1$$

and since all constant parameters in this second-order linear differential equation are strictly positive, this defines an asymptotically stable linear system. Thus, $x_1(t), \dot{x}_1(t)$ converge exponentially to zero as $t \longrightarrow +\infty$, and it follows that Subsystem (44) is asymptotically stable. The transient behavior of x_1 can be analyzed via the damping coefficient of the above differential equation. The natural frequency of this second-order linear system is

$$\bar{\varpi}_1 = \sqrt{\frac{m_1 \varpi_1^2}{m_1 + c_1 \tau_1}}$$

and its damping coefficient ξ_1^* is defined by the relation

$$2\xi_1^* \sqrt{\frac{m_1 \varpi_1^2}{m_1 + c_1 \tau_1}} = \frac{c_1 + k_2 \tau_1}{m_1 + c_1 \tau_1}$$

Thus,

$$2\xi_1^* \varpi_1 \sqrt{m_1} = \frac{c_1 + k_2 \tau_1}{\sqrt{m_1 + c_1 \tau_1}}$$

which implies that

$$(c_1 + k_2 \tau_1)^2 - 4(\xi_1^*)^2 \varpi_1^2 m_1 (m_1 + c_1 \tau_1) = 0$$

Since τ_1 defined by (20) is the positive solution of the second-order polynomial equation

$$(c_1 + k_2 \tau_1)^2 - 4(\xi_1)^2 \varpi_1^2 m_1 (m_1 + c_1 \tau_1) = 0$$

it follows that $\xi_1^* = \xi_1$. ∎

6 Conflict of Interest

The authors declare that they have no conflict of interest

7 Data Availability Statements

All data generated or analysed during this study are included in this published article (and its supplementary information files)

References

[1] A. Della Gatta, L. Tannelli, and M. Pisaturo. A survey on modeling and engagement control for automotive dry clutch. *Mechatronics*, 55:63–75, 2018.

[2] A. Papinniemi, J. Lai, J. Zhao, and L. Loader. Brake squeal: a literature review. *Applied Acoustics*, 63:391–400, 2002.

[3] A. Saha, B. Bhattacharya, and P. Wahi. A comparitive study on the control of friction-driven oscillations by time- delayed feedback. *Nonlinear Dynamics*, 60:15–37, 2010.

[4] B. Armstrong-Helouvry and B. Amin. Pid control in the presence of static friction:a comparison of algebraic and describing function analysis. *Automatica*, 32:679–692, 1996.

[5] B. Armstrong-Helouvry, P. Dupont, and C. Canudas de Wit. A survey of models, analysis tools, and compensation methods for the control of machines with friction. *Automatica*, 30:1083–1138, 1994.

[6] B. Bergeot, S. Berger, and S. Bellizzi. Mode coupling instability mitigation in friction systems by means of nonlinear energy sinks: numerical ighlighting and local stability analysis. *Journal of Vibration and Control*, 24(15):3487–3511, 2017.

[7] B.A. Bucci, D.G. Cole, S.J. Ludwick, and J.S. Vipperman. Nonlinear control algorithm for improving settling time in systems with friction. *IEEE Transaction on Control Systems Technology*, 21:1365–1374, 2013.

[8] B.Bergeot, S. Bellizzi, and S. Berger. Mitigation of friction-induced vibrations in braking systems:prediction of the mitigation limit. In *28th International Conference on Noise and Vibration Engineering (ISMA2018)*, pages 3315–3330, Louvain, Belgium, September 2018.

[9] B.Delibas and B.Koc. A method to realize low velocity movability and eliminate friction induced noise in piezoelectric ultrasonic motors. *IEEE/ASME Transactions on Mechatronics*, 25(6):2677–2687, 2020.

[10] C. Chevennement-Roux, T. Dreher, E. Aubry, J.-P. Lainé, and L. Jézéquel. Flexible wiper system dynamic instabilities: modeling and experimental validation. *Experimental Mechanics*, 47:201–210, 2007.

[11] C. Zhen, S. Jiffri, D. Li, J. Xiang, and J. E. Mottershead. Feedback linearisation of nonlinear vibration problems: A new formulation by the method of receptances. *Mechanical Systems and Signal Processing*, 98:1056–1068, 2018.

[12] C. Zheng, Y.Su, and P. Mercorelli. Faster positioning of one degree-of-freedom mechanical systems with friction and actuator saturation. *Journal of Dynamic Systems, Measurement and Control, Trans. of the ASME*, 141(6), 2019.

[13] C. Zheng, Y.Su, and P. Mercorelli. A simple nonlinear pd control for faster and high-precision positioning of servomechanisms with actuator saturation. *Mechanical Systems and Signal Processing*, 121:215–226, 2019.

[14] C. Zheng, Y.Su, and P. Mercorelli. Simple saturated relay nonlinear pd control for uncertain motion systems with friction and actuator constraint. *IET Control Theory Applications*, 13(12):1920–1928, 2019.

[15] S. Chatterjee. Non-linear control of friction-induced self-excited vibration. *International Journal of Nonlinear Mechanics*, 42:459–469, 2007.

[16] S. Chatterjee. Time-delayed feedback control of friction-induced instability. *International Journal of Nonlinear Mechanics*, 42:1143–1127, 2007.

[17] F. Chen. Disc brake squeal: An overview. *International Journal Vehicle Design*, 51:167–172, 2009.

[18] E. Sarrouy, O. Dessombz, and J.-J. Sinou. Stochastic study of non-linear self-excited system with friction. *European Journal of Mechanics A/Solids*, 40(2):1–10, 2013.

[19] G. Ouenzerfi, F. Massi, E. Renault, and Y. Berthier. Squeaking friction phenomena in ceramic hip endoprosthesis: Modeling and experimental validation. *Mechanical Systems and Signal Processing*, 58-59:87–100, 2015.

[20] G-P. Ostermeyer, M. Muller, S. Brumme, and T. Srisupattarawanit. Stability analysis with an nvk minimal model for brakes under consideration of polymorphic uncertainty of friction. *Vibration*, 2:135–156, 2019.

[21] G.Ievgen and P.Stefan. Pfc-based control of friction-induced instabilities in drive systems. *Machines*, 9(7), 2021.

[22] H. Ouyang, W. Nack, Y. Yuan, and F. Chen. Numerical analysis of automative disc brake squeal: a review. *International Journal of Vehicle Noise and Vibration*, 1:207–231, 2005.

[23] J. Hultèn. Drum brake squeal-a self exciting mechanism with constant friction. In *In the SAE truck and bus meeting, 1993, Detroit, MI, USA SAE paper*, page 932965, 1993.

[24] R.A. Ibrahim. Friction-induced vibration, chatter, squeal, and chaos part 1: mechanics of contact and friction. *Am Soc Mech Eng Appl Mech Rev*, 47(7):209–226, 1994.

[25] R.A. Ibrahim. Friction-induced vibration, chatter, squeal, and chaos part 2: dynamics and modeling. *Am Soc Mech Eng Appl Mech Rev*, 47(7):227–263, 1994.

[26] J. Das and A. K. Mallik. Control of friction driven oscillation by time-delayed state feedback. *Journal of Sound and Vibration*, 297(3-5):578–594, 2006.

[27] J-J. Sinou and L. Jézéquel. Mode coupling instability in friction-induced vibrations and its dependency on system parameters including damping. *European Journal of Mechanical A/Solid*, 26:107–122, 2007.

[28] J.Awrejcewicz and P. Olejnik. Numerical and experimental investigations of simple non-linear system modeling a girling duo-servo brake mechanism. In *In: ASME 2003 Design Engineering Technical Conferences and Computers and Information in Engineering Conference*, Chicago, Illinois, September 2003.

[29] J.Awrejcewicz and P. Olejnik. Analysis of dynamic systems with various friction laws. *Applied Mechanics Reviews*, 58:389–411, 2005.

[30] K. Nakano and S. Maegawa. Safety-design criteria of sliding systems for preventing friction-induced vibration. *Journal of Sound and Vibration*, 324:539–555, 2009.

[31] K. Popp and M. Rudolph. Vibration control to avoid stick-slip motion. *Journal of Vibration and Control*, 10:1585–1600, 2004.

[32] K. V. Singh and H. Ouyang. Pole assignment using state feedback with time delay in friction-induced vibration problems. *Acta Mechanica*, 224(3):645–656, 2012.

[33] K.A. Cunefare and A.J. Graf. Experimental active control of automotive disk brake rotor using dither. *Journal of Vibration and Control*, 250:579–590, 2002.

[34] H.K. Khalil. *Nonlinear Systems*. Pearson Education. Prentice Hall, 2002.

[35] L. Nechak and J-J. Sinou. Hybrid surrogate model for the prediction of uncertain friction-induced instabilities. *Journal of Sound and Vibration*, 126:122–143, 2017.

[36] L. Nechak, S. Berger, and E. Aubry. Wiener askey and wiener haar expansions for the analysis and prediction of limit cycle oscillations in uncertain nonlinear dynamic friction systems. *ASME Journal of Computational and Nonlinear Dynamics*, 9(2):021007, 2014.

[37] L.Nechak. Robust nonlinear control synthesis by using centre manifold-based reduced models for the mitigating of friction-induced vibration. *Nonlinear Dynamics*, 108(3):1885–1901, 2022.

[38] M. G. Tehrani and H. Ouyang. Receptance-based partial pole assignment for asymmetric systems using state-feedback. *Shock and Vibration*, 19(5):1135–1142, 2012.

[39] M. Yoshihiro and I. Makoto. Rolling friction model-based analyses and compensation for slow settling response in precise positioning. *IEEE Transactions on Industrial Electronics*, 60(12):5841–5853, 2013.

[40] N. M. Kindkaid, O. M. O'Reilly, and P. Papadopoulos. Automative disc brake squeal. *Journal of Sound and Vibration*, 267:105–166, 2003.

[41] N. M. Kindkaid, O. M. O'Reilly, and P. Papadopoulos. On the transient dynamics of a multi-degree-of-freedom friction oscillator: a new mechanism for disc brake noise. *Journal of Sound and Vibration*, 287:901–917, 2005.

[42] L. Nechak. Nonlinear control of friction-induced limit cycle oscillations via feedback linearization. *Mechanical Systems and Signal Processing*, 126:264–280, 2019.

[43] L. Nechak. Nonlinear state observer for estimating and controlling of friction-induced vibrations. *Mechanical Systems and Signal Processing*, 4:3917–3933, 2020.

[44] L. Nechak. Robust nonlinear control of mode-coupling-based vibrations by using high-gain observer and sliding-mode controller. *Journal of Dynamical System Measurement and Control*, 143:14 pages, 2021.

[45] N.Hoffmann and L.Gaul. Effects of damping on mode-coupling instability in friction induced oscillations. *ZAMM-Journal of Applied Mathematics and Mechanics/Zeitschrift für Angewandte Mathematik und Mechanik: Applied Mathematics and Mechanics*, 83(8):524–534, 2003.

[46] H. Ouyang. Prediction and assignment of latent roots of damped asymmetric systems by structural modifications. *Mechanical Systems and Signal Processing*, 23(6):1920–1930, 2009.

[47] P.K. Sahoo and S. Chatterjee. Effect of high-frequency excitation on friction induced vibration caused by the combined action of velocity-weakening and mode-coupling. *Journal of Vibration and Control*, 26(9-10):735–746, 2020.

[48] R. Konowrocki, T.Szolc, A. Pochanke, and A. Pręgowska. An influence of the stepping motor control and friction models on precise positioning of the complex mechanical system. *Mechanical System Signal Processing*, 70-71:397–413, 2013.

[49] R. P. Jarvis and B. Mills. Vibrations induced by dry friction. *Proceedings of the Institution of Mechanical Engineers*, 178(1):847–857, 1963.

[50] R.D. Savant, S. Y. Gajjal, and V. G. Patil. Review on disc brake squeal. *International Journal of Engineering Trends and Technology*, 9:605–608, 2014.

[51] R.H.A. Hensen, M.J.G. Van De Molengraft, and M. Steinbuch. Friction-induced hunting limit cycles: an event mapping approach. In *Proceeding of the 2002 American Control Conference, Anchorage, AK*, pages 2267–2272, 2002.

[52] S. Y. Liu, J. T.Gordon, and A. Ozbek. Journal of aircraft. *Proceedings of the Institution of Mechanical Engineers*, 35(4):623–630, 1998.

[53] S.M. Hashemi-Dehkordi, M. Mailah, and A.R. Abu-Bakar. Suppressing friction-induced vibration due to negative damping and mode coupling effects using active force control. *Australian Journal of Basic and Applied Sciences*, 4:3917–3933, 2010.

[54] T. Jearsiripongkul and D. Hochlenert. Disk brake squeal: Modeling and active control. In *2006 IEEE Conference on Robotics, Automation and Mechatronics*, pages 1–5, 2006.

[55] T.Baumberger and C.Caroli. Solid friction from stick–slip down to pinning and aging. *Advances in Physics*, 55(3-4):279–348, 2006.

[56] V. Pilipchuk, P. Olejnik, and J. Awrejcewicz. Transient friction-induced vibrations in a 2-dof model of brakes. *Journal of Sound and Vibration*, 344:297–312, 2015.

[57] Y. Liang, H. Yamaura, and H. Ouyang. Active assignment of eigenvalues and eigen-sensitivities for robust stabilization of friction-induced vibration. *Mechanical Systems and Signal Processing*, 90:254–267, 2017.

[58] Y.Jianyong, D.Wenxiang, and J.Zongxia. Adaptive control of hydraulic actuators with lugre model-based friction compensation. *IEEE Transactions on Industrial Electronics*, 62(10):6469–6477, 2015.

[59] Y.Su, C.Zheng, and P.Mercorelli. Velocity-free friction compensation for motion systems with actuator constraint. *Mechanical Systems and Signal Processing*, 148:107132, 2021.

[60] Z. Zhang, S. Oberst, and J.C.S. Lai. On the potential of uncertainty analysis for prediction of brake squeal propensity. *Journal of Sound and Vibration*, 377:123–132, 2016.

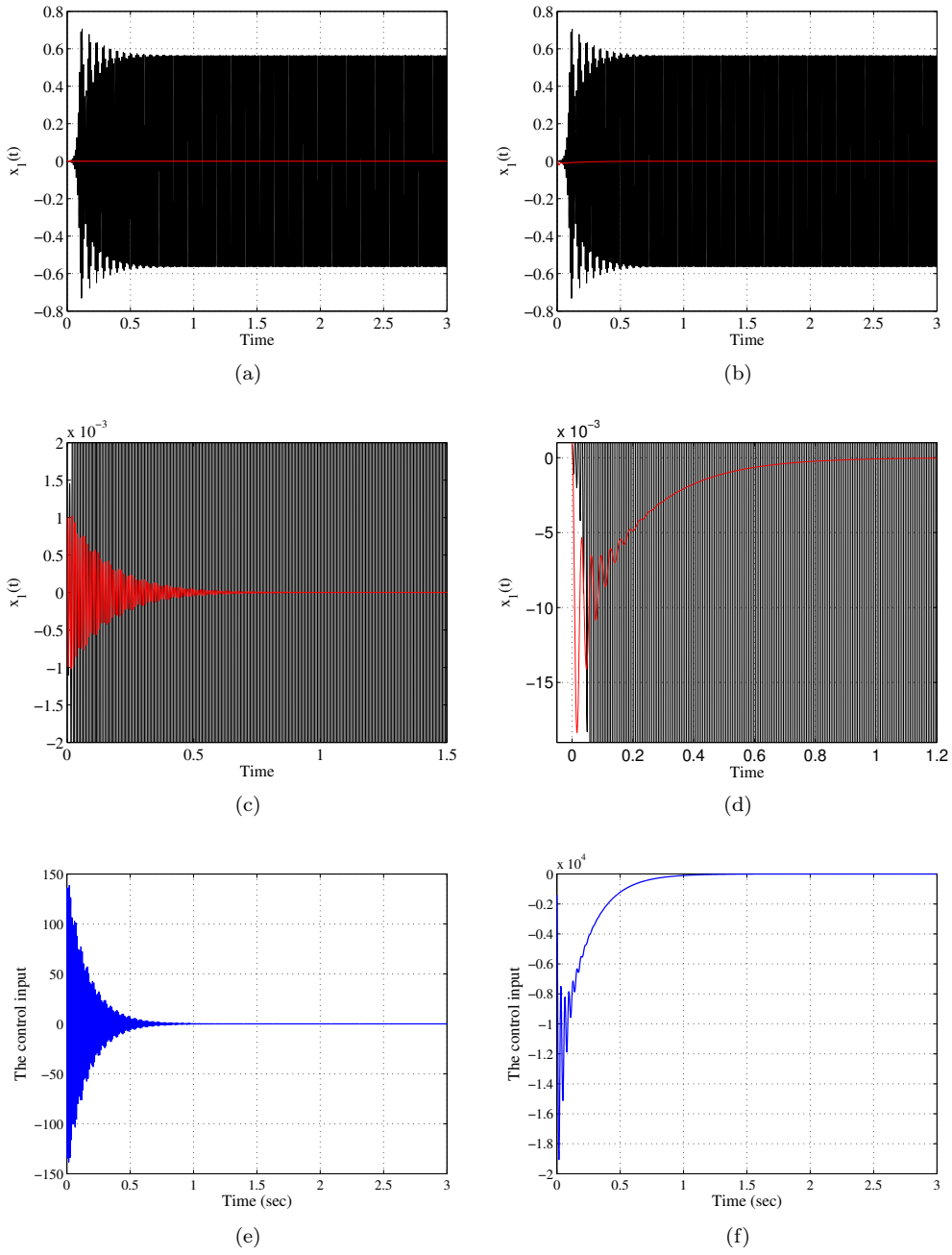

Figure 3: Time evolution of the displacement x_1: (a,b) Non-controlled solution (dark line) and controlled solution by feedback linearization, i.e., eq. (3) (red line), (c,d) Zoom on the transient of $x_1(t)$, (e) Control input corresponding to poles placed in the left half-plane at a moderate distance from the imaginary axis, (f) Control input corresponding to poles placed very left in the left half-plane.

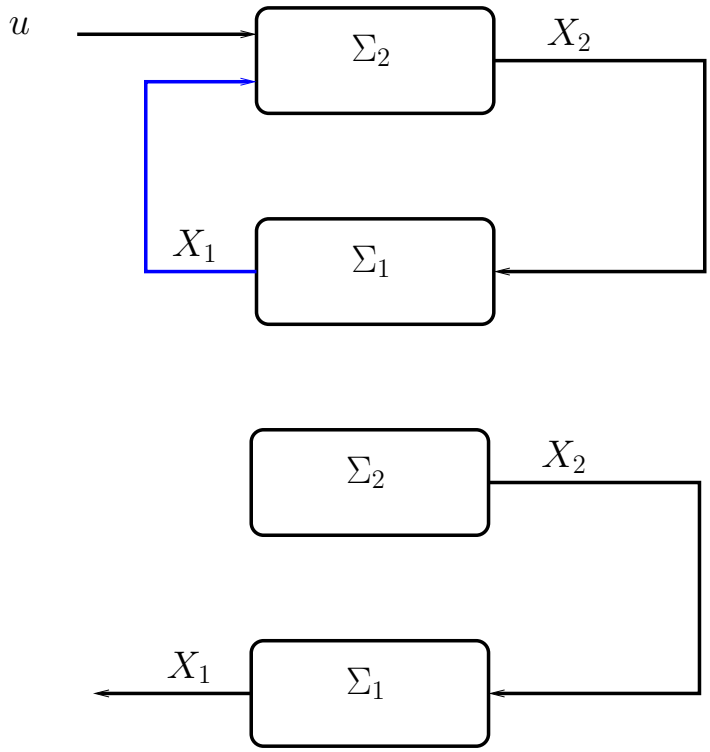

Figure 4: Block diagram representation of the control system (upper), and of the closed-loop system of Proposition (1) (lower)

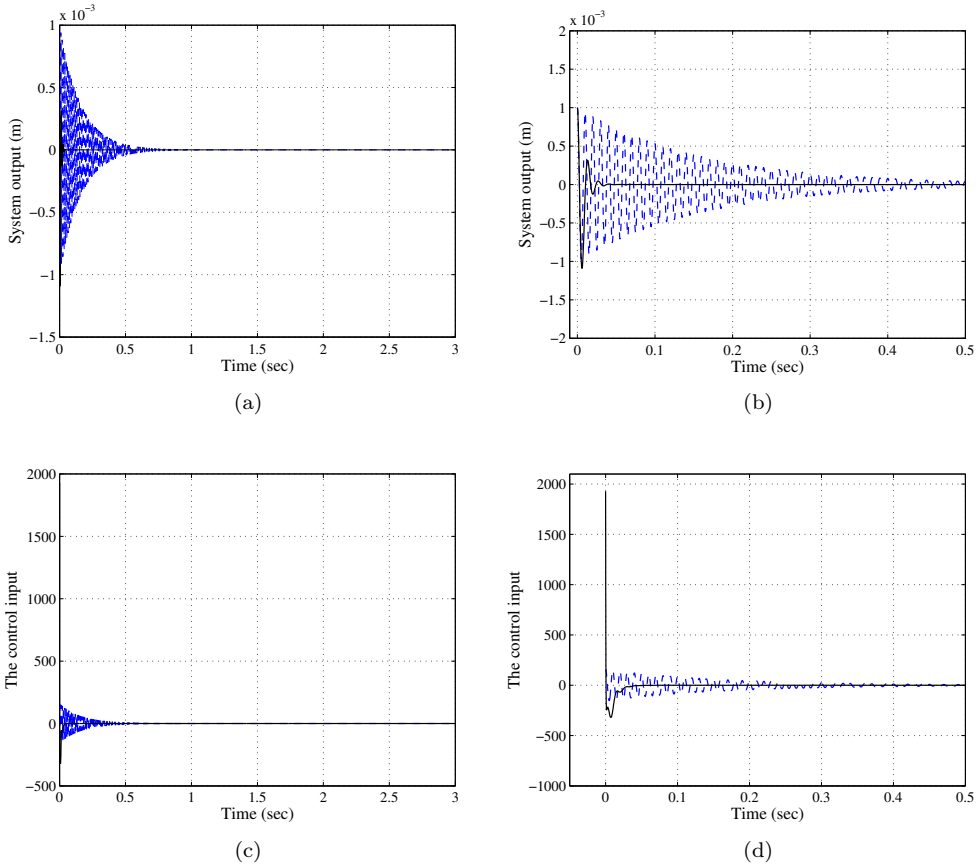

Figure 5: (a)- Controlled displacement $X_1(t)$, (b)-Zoom on the transient of X_1, (c)-Control input, (d)-Zoom on the transient of the control input. Solid line: proposed control solution (11), dashed line: solution based on feedback linearization (3)

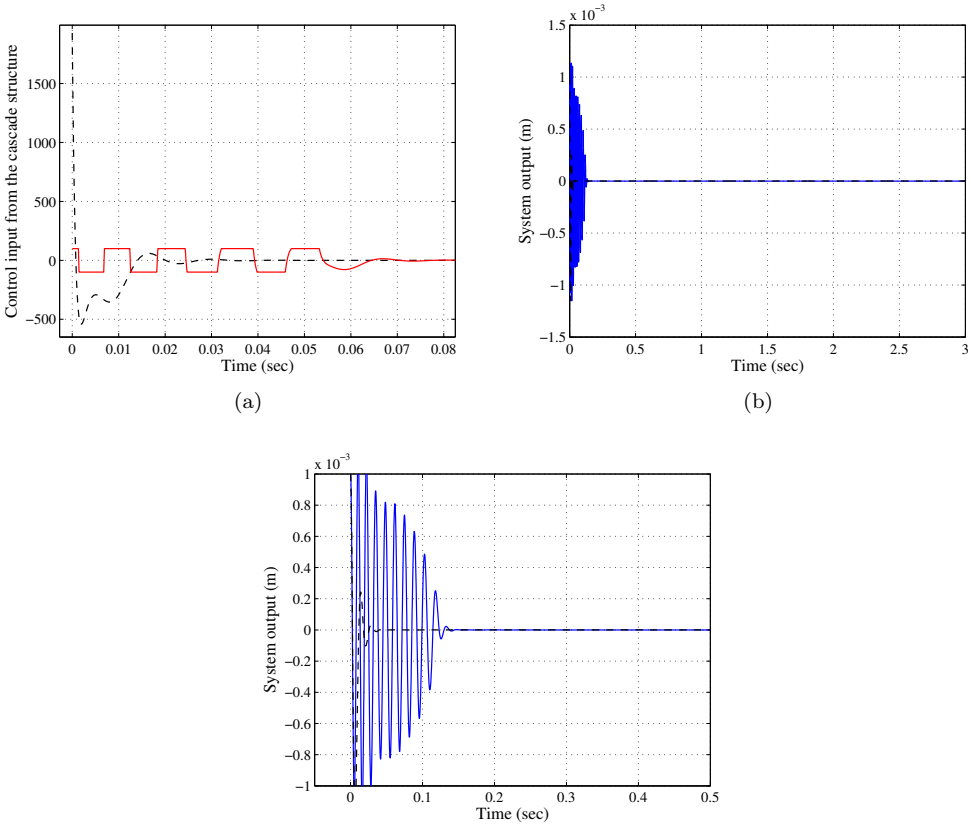

Figure 6: (a)-Zoom on the control input, (b)-Controlled displacement X_1, (c)-Zoom on the transient of X_1. Dashed line: without saturation, solid line: with saturation

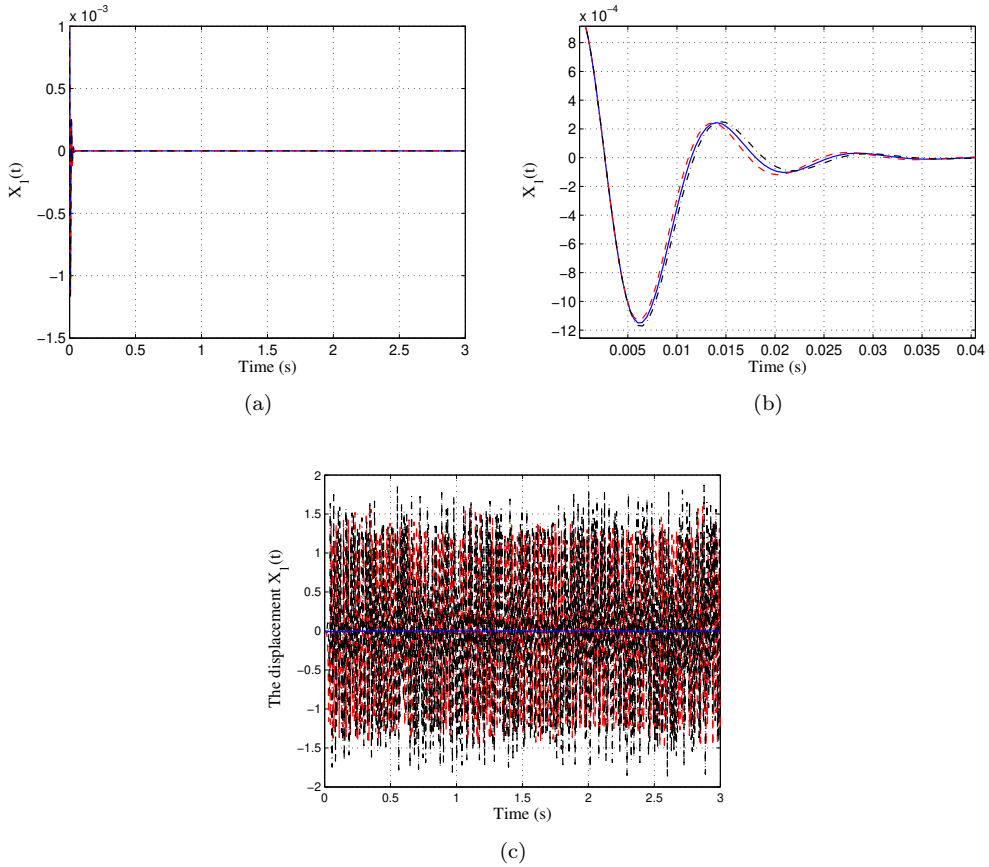

Figure 7: (a)- Displacement X_1 with the proposed control solution, i.e., (11) and (12), (b)- Zoom on the transient of X_1 with this solution, (c)-Solution based on feedback linearization, i.e., (3) and (4). Solid line: nominal value ($\mu = 0.4$), dashed line: minimum value ($\mu = 0.38$), dashed-dot line: maximum value ($\mu = 0.42$)

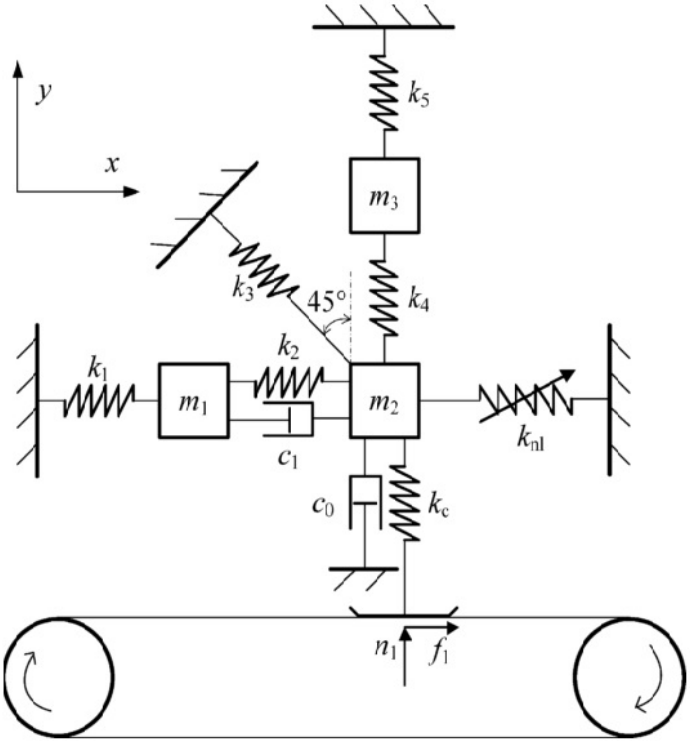

Figure 8: Mechanical system submitted to mode-coupling instabilities

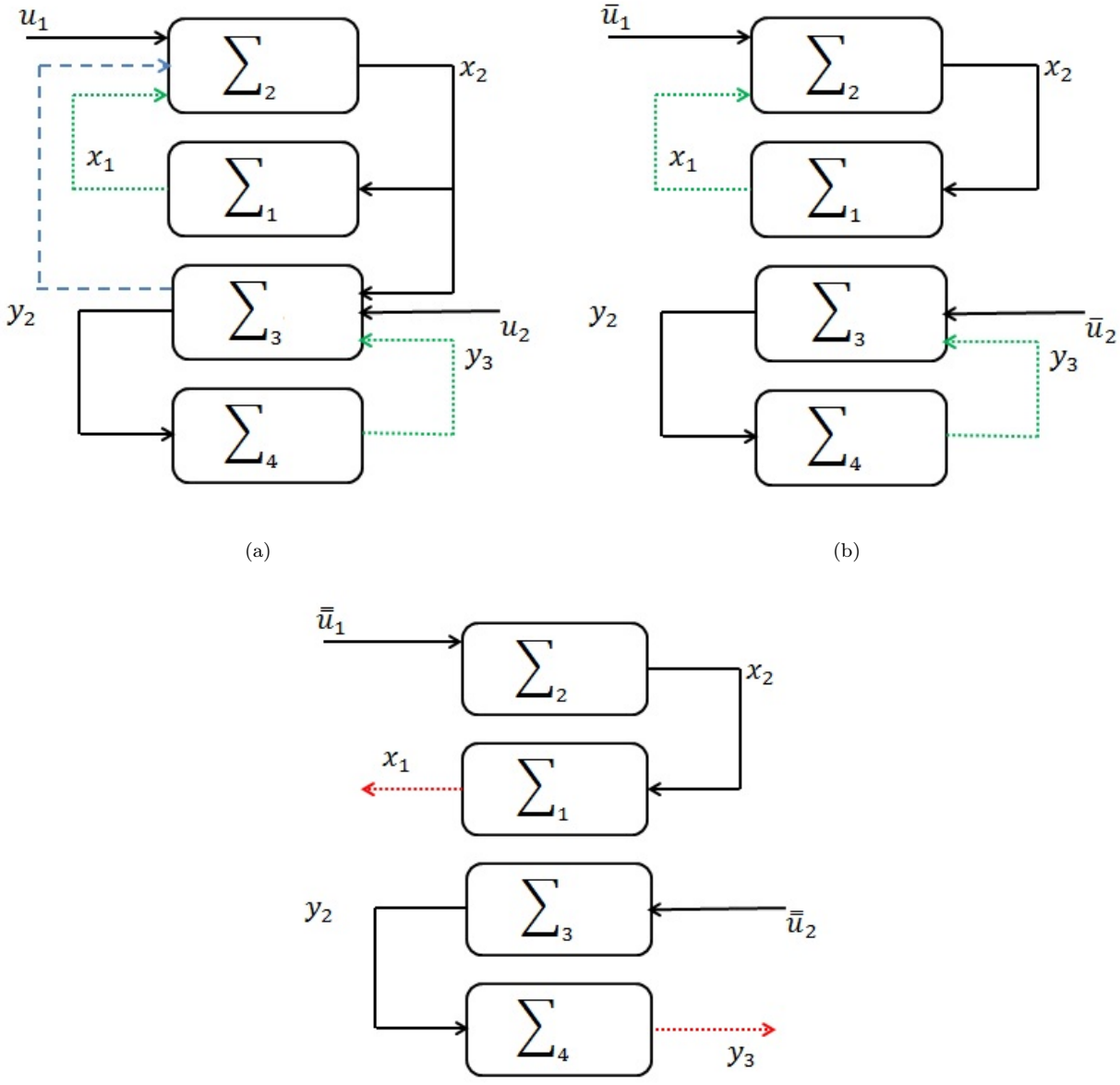

(a) (b)

(c)

Figure 9: (a)-Original system, (b)- Intermediary configuration, (c)-Cascade configuration

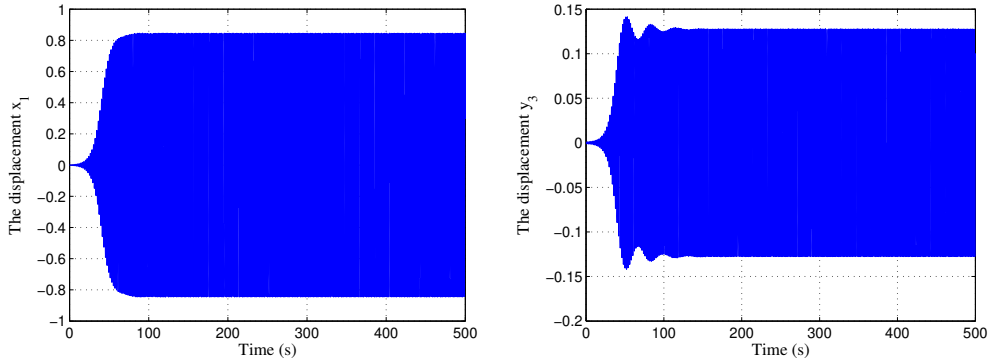

(a) (b)

Figure 10: Mode-coupling based vibrations in System (8)

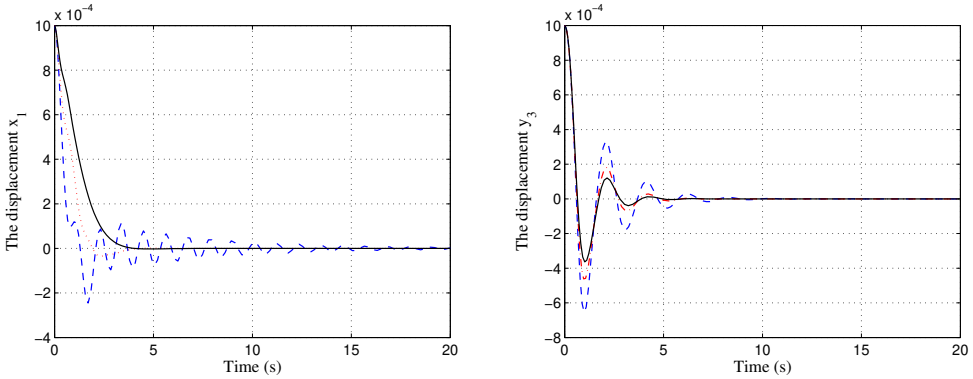

(a) (b)

Figure 11: Controlled system displacements x_1 and y_3 corresponding to different damping rates. Dashed line: $\xi_i = 0.3$, Dashed-dot line: $\xi_i = 0.5$, Solid line: $\xi_i = 0.7$

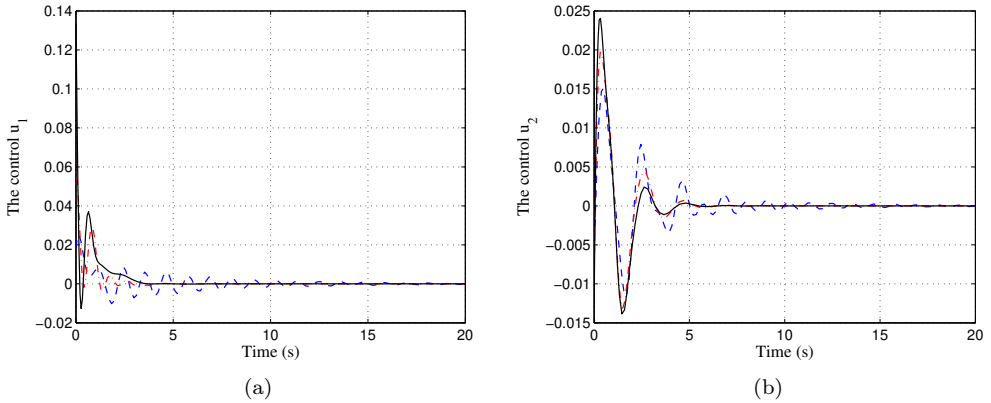

(a) (b)

Figure 12: Control signals corresponding to different damping rates. Dashed line: $\xi_i = 0.3$, Dashed-dot line: $\xi_i = 0.5$, Solid line: $\xi_i = 0.7$

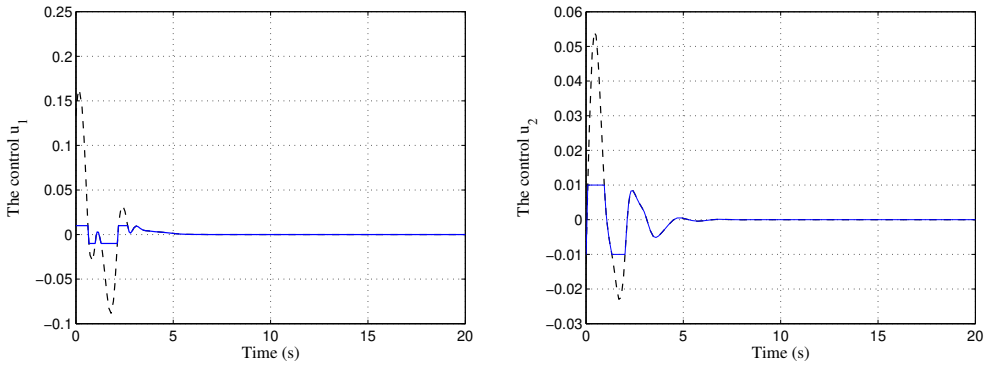

(a) (b)

Figure 13: Control signal corresponding to $\xi_i = 0.7$. Dashed line: Non-saturated control, Solid line: saturated control

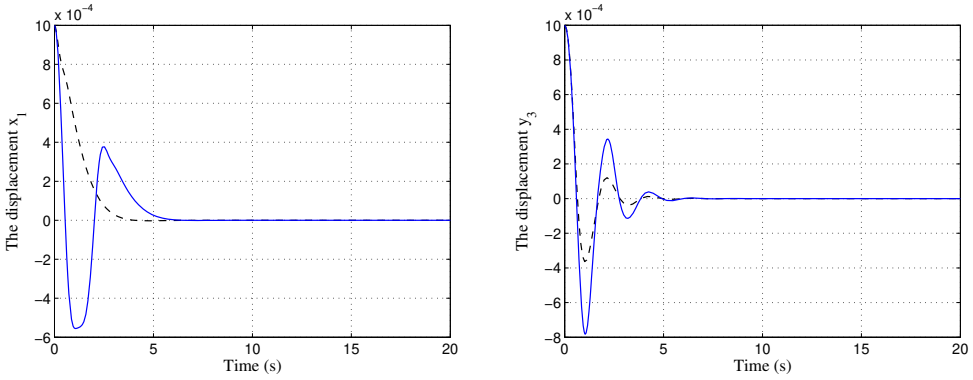

(a) (b)

Figure 14: Controlled displacements x_1 and y_3 corresponding to $\xi_i = 0.7$. Dashed line: obtained with a non-saturated control, Solid line: obtained with a saturated control

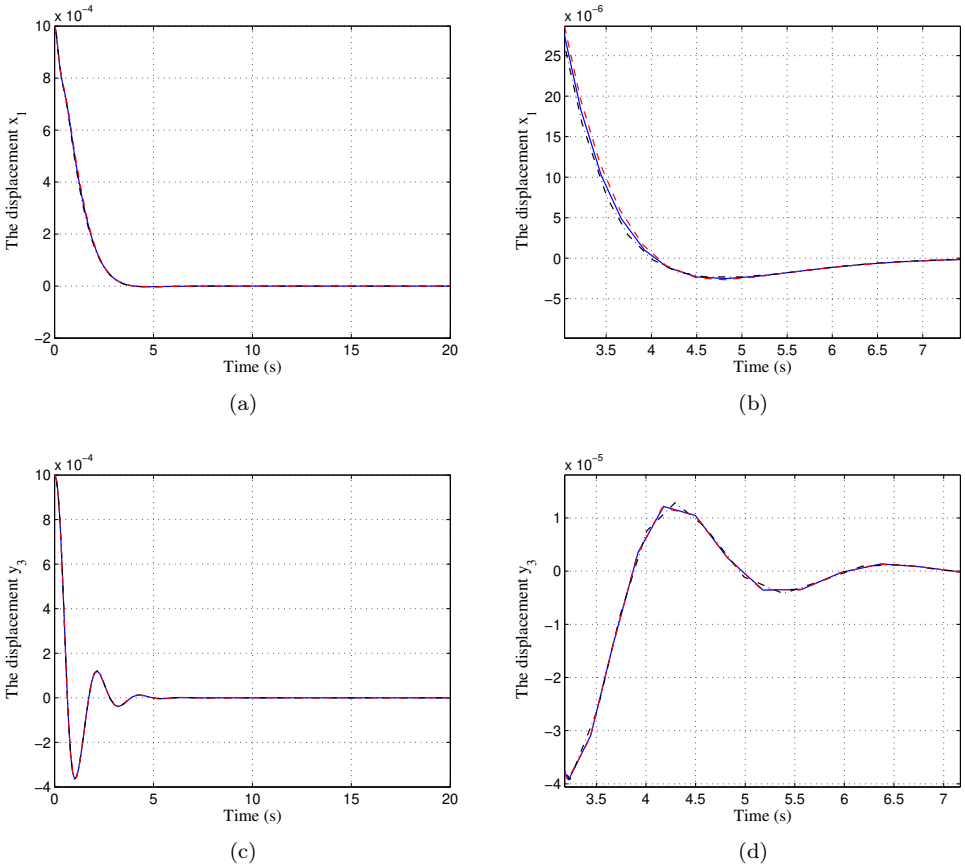

Figure 15: (a,c): Displacements x_1 and y_3 obtained with the proposed solution (17)-(19)-(21), (b,d): Zoom on the transients of x_1 and y_3. Solid line: nominal value ($\mu = 0.5$), dashed line: minimal value ($\mu = 0.45$), dashed-dot line: maximal value ($\mu = 0.55$)